https://doi.org/10.1007/s11629-018-5153-5

Thermal dynamics of the permafrost active layer under increased precipitation at the Qinghai-Tibet Plateau

LI De-sheng [1] https://orcid.org/0000-0002-9752-338X; e-mail: ridson319@sjtu.edu.cn

WEN Zhi [2*] https://orcid.org/0000-0002-2895-7723; e-mail: wenzhi@lzb.ac.cn

CHENG Qian-gong [3] https://orcid.org/0000-0002-1874-357X; e-mail: chengqiangong@home.swjtu.edu.cn

XING Ai-guo [1] https://orcid.org/0000-0002-9388-7012; e-mail: xingaiguo@sjtu.edu.cn

ZHANG Ming-li [4] https://orcid.org/0000-0002-4350-4781; e-mail: mingli_0919@126.com

LI An-yuan [5] https://orcid.org/0000-0003-1821-7630; e-mail: anyuanli1013@lzb.ac.cn

**Corresponding author*

[1] *State Key Laboratory of Ocean Engineering, Shanghai Jiao Tong University, Shanghai 200240, China*

[2] *State Key Laboratory of Frozen Soil Engineering, Northwest Institute of Eco-Environmental and Resources, CAS, Lanzhou 730000, China*

[3] *Department of Geological Engineering, Southwest Jiaotong University, Chengdu 614202, China*

[4] *Department of Civil Engineering, Lanzhou University of Technology, Lanzhou 730050, China*

[5] *Department of Civil Engineering, Shaoxing University, Shaoxing 312099, China*

Citation: Li DS, Wen Z, Cheng QG, et al. (2019) Thermal dynamics of the permafrost active layer under increased precipitation at the Qinghai-Tibet Plateau. Journal of Mountain Science 16(2). https://doi.org/10.1007/s11629-018-5153-5.

© Science Press, Institute of Mountain Hazards and Environment, CAS and Springer-Verlag GmbH Germany, part of Springer Nature 2019

Abstract: Precipitation has a significant influence on the hydro-thermal state of the active layer in permafrost regions, which disturbs the surface energy balance, carbon flux, ecosystem, hydrological cycles and landscape processes. To better understand the hydro-thermal dynamics of active layer and the interactions between rainfall and permafrost, we applied the coupled heat and mass transfer model for soil-plant-atmosphere system into high-altitude permafrost regions in this study. Meteorological data, soil temperature, heat flux and moisture content from different depths within the active layer were used to calibrate and validate this model. Thereafter, the precipitation was increased to explore the effect of recent climatic wetting on the thermal state of the active layer. The primary results demonstrate that the variation of active layer thickness under the effect of short-term increased precipitation is not obvious, while soil surface heat flux can show the changing trends of thermal state in active layer, which should not be negligible. An increment in year-round precipitation leads to a cooling effect on active layers in the frozen season, i.e. verifying the insulating effect of "snow cover". However, in the thawed season, the increased precipitation created a heating effect on active layers, i.e. facilitating the degradation of permafrost. The soil thermal dynamic in single precipitation event reveals that the precipitation event seems to cool the active layer, while compared with the results under increased precipitation, climatic wetting trend has a different influence on the permafrost evolution.

Received: 04 August 2018
Revised: 12 November 2018
Accepted: 14 November 2018

Keywords: Active layer; Precipitation;·Qinghai-Tibet plateau; Hydro-thermal dynamic

Introduction

The top layer of the ground subject to annual thawing and freezing in permafrost regions is defined as the active layer (Zhou 2013). The active layer responds quickly to climate change, which leads to dramatic changes in the physical and chemical properties of the soil, as well as its hydro-thermal dynamics and nitrogen and carbon cycles (Koven et al. 2011; Nelson et al. 2004). Climate change has a significant influence on the active layer, i.e. causing the extensive degradation of permafrost all over the world (Iijima et al. 2010; Jin et al. 2007; Schuur et al. 2015; Stendel and Christensen 2002; Zimov and Schuur 2006). Furthermore, the Qinghai-Tibet Highway and Qinghai-Tibet Railway have been constructed across the Qinghai-Tibet Plateau (Q-T Plateau) distributed with discontinuous permafrost (Ma et al. 2008). The hydro-thermal transport during the freeze-thaw cycle significantly influences linear cold region engineering (Kroener et al. 2014).

Previous studies focused more on the effect of global warming on the permafrost active layer, and the research results showed that the active layer responds positively to global warming (Anisimov et al. 1997; Stendel and Christensen 2002), whereas less attention was paid to the effects of increased precipitation. Compared with the influence of air temperature changes, the effect of precipitation changes on the permafrost was not significant (Hu et al. 2015; Zhao et al. 2013). Nevertheless, from monitoring data it is found that the increasing precipitation did influence the permafrost active layer (Wen et al. 2014; Wu et al. 2015; Zhu et al. 2011).

In the Chinese Qinghai-Tibet Plateau, the influence of precipitation on the hydro-thermal dynamics in different seasons varied distinctly: the precipitation in the frozen season tends to cool the active layer. Furthermore, the insulating effect of snow cover promote positive development of permafrost in winter (Zhang 2005; Ling and Zhang 2003; Stieglitz et al. 2003; Zhang et al. 2001). Opinions divide concerning the effect of rainfall in the thawed season. Using monitoring data, Wu et al. (2015) suggested that increased precipitation in summer warmed the active layer and increased the thickness of the active layer. Zhou et al. (2017) concluded that precipitation, together with a warming climate, led to the degradation of grassland. Through the comparison of the active layer's thermal state between pre- and post-rainfall events, Wen et al. (2014) found that the rainfall events in summer chilled the active layer. Kokelj et al. (2015) believed that greater frequency and magnitude of precipitation events can affect the geomorphic evolution of permafrost landscapes by increasing the heat transfer and accelerating thermal erosion. The effect of extreme precipitation events is also significant for the thermal state of the active layer. Zhu et al. (2017) indicated that the precipitation events with higher rainfall quantities show a greater influence on the hydro-thermal state of the active layer than rainfall events with a longer duration.

Several numerical simulation models have been used in order to analyze the thermal condition and variation of active layer thickness in response to precipitation changes in the Q-T Plateau. These simulations improved the understanding of the hydro-thermal transfer process and the mechanism of soil water infiltration and evaporation. This research involves a predictable changing trend of permafrost active layer thermal state in response to increased precipitation. Little progress has been made in this area before, qualitatively or quantitatively. Hence, in this study the simulated thermal state of the active layer in the Q-T Plateau under increased precipitation was discussed.

In this study, the CoupModel published by Jansson and Karlberg (2001) was first applied to the simulation of the hydro-thermal dynamics of the active layer in the Beiluhe area. The meteorological and hydro-thermal data from the study site are used to validate and calibrate the model. Thereafter, conditions with increased precipitation to different extents are imported to explore the effect of changing precipitation on the thermal state of permafrost active layer in the Q-T Plateau.

1 Monitoring Data

1.1 Study site

The field observation site is located between Fenghuo Mountains and the Kekexili volcanic area in the Qinghai-Tibet Plateau, the ground is flat with an elevation of 4620 m (34.51°N and 92.56°E) (Figure 1). The annual mean air temperature and accumulated precipitation amounts in 2013 are -3.29℃ and 318.8 mm, respectively. The vegetation in this region is alpine meadow with a height of less than 0.1 m.

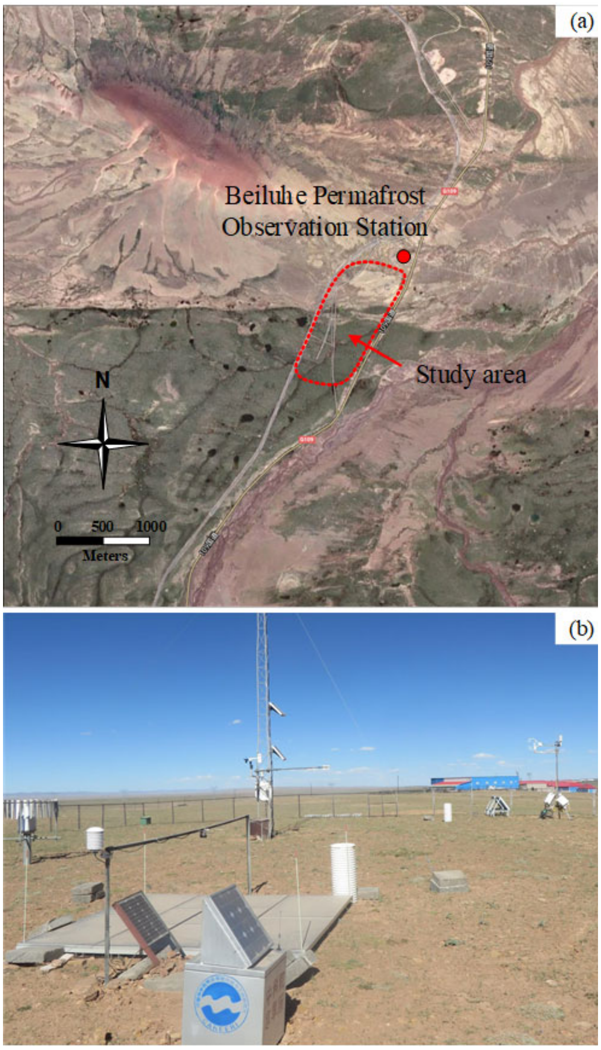

Figure 1 Overview of the study area in Beiluhe area at Qinghai-Tibet Plateau.

1.2 Soil profile

In this model, the compartment number is 20 and the depth of the lower boundary is 10.2 m. The shallow compartments are set to correspond to those compartments divided by hydro-thermal sensors at the monitoring site, namely, the midpoint of each compartment in the model is the position where the sensor was installed (Figure 2). The deep compartments were separated at the intervals of 1 m from 2.2 m to 10.2 m, which could more effectively simulate the changes in the permafrost active layer. The thickness of the humus layer is less than 0.1 m.

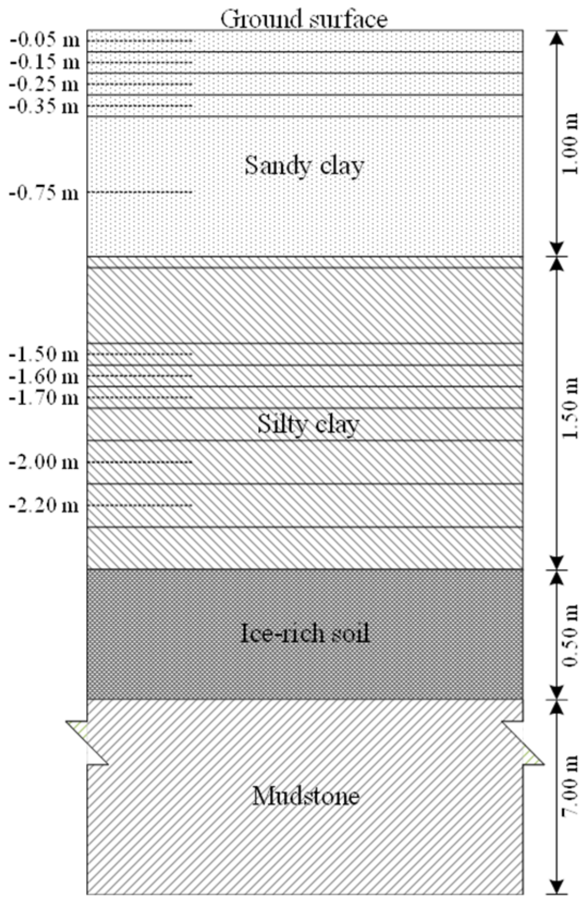

Figure 2 Vertical distributions of soil layer and temperature sensors at ten different depths.

1.3 Data

The air temperature, precipitation, relative humidity, global radiation, net radiation and wind speed at 2.20 m above the ground were measured every half hour at the meteorological station in the Beiluhe area from January 1st 2013 to December 31st 2013 (Figure 3). Soil temperature and water content were measured at depths of 0.05, 0.15, 0.25, 0.35, 0.75, 1.50, 1.60, 1.70, 2.00 and 2.20 m (Figure 2). The soil heat flux was measured at the depths of 0.05 m and 0.15 m. All data were recorded once every 30 minutes. The calculation

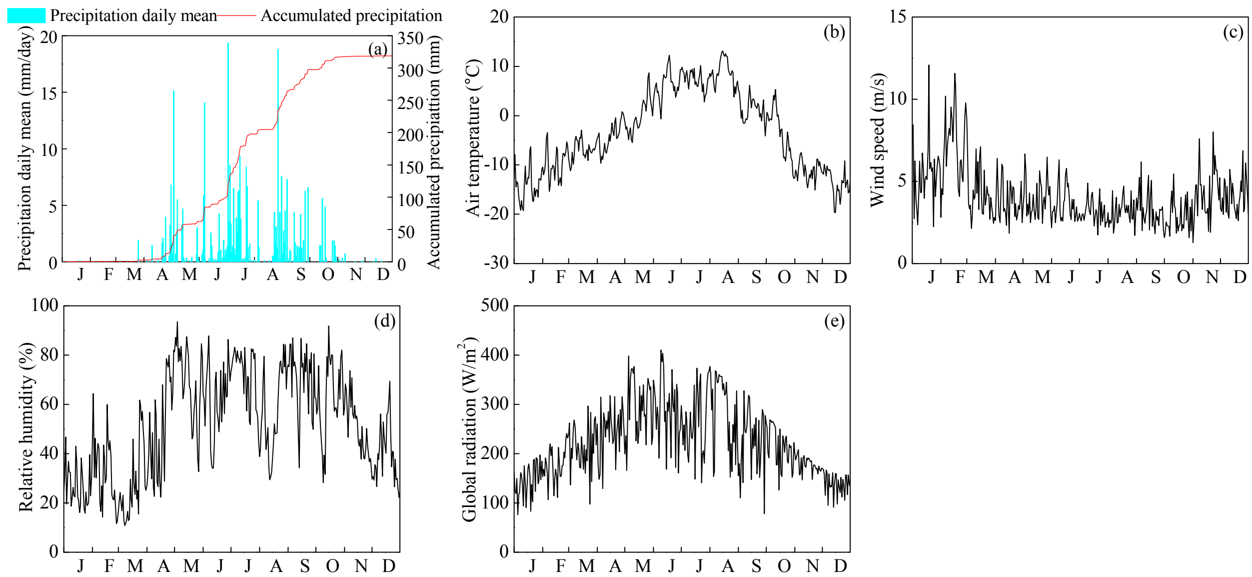

Figure 3 Measured atmosphere data from Beiluhe atmospheric station in 2013. (a) Daily mean precipitation and accumulated precipitation; (b) air temperature at 2 m above the ground surface; (c) wind speed at 2 m above the ground surface; (d) relative humidity at 2 m above the ground surface; (e) global radiation.

step in this model is one day, so the data used in this study is the daily mean values.

2 Model Validation

In this study, the atmospheric driving data in 2013 was applied as input data. Then, the simulated hydro-thermal alternation was calibrated and compared with the measured data in 2013.

2.1 Model description

The CoupModel (Jansson and Karlberg 2001) is the updated and modified version evolved from the SOIL (Jansson 1991) and SOILN (Johnsson and Jansson 1993) Model, which was published by Jansson and Karlberg. The new version could be applied to any type of terrestrial system, including semi-arid regions (Rockström et al. 1998) and permafrost regions (Hollesen et al. 2011). This model concentrates on soil physics, which couples water flow using the Richard equation and heat flow using the Fourier equation for soil-plant-atmosphere systems in a one-dimensional domain. The best merit of this model is that the desirable result could be achieved through the input of finite data.

Brief descriptions of the important heat and water modules used in this model are shown below:

(a) Soil heat process.

The heat flow in this model is expressed as the sum of conduction, liquid and vapor convection:

$$q_h = -k_h \frac{\partial T}{\partial z} + C_w T q_w + L_v q_v \qquad (1)$$

where the indices h, w and v mean heat, liquid and vapor water, respectively, q is the flux, T is the soil temperature (℃), C is the heat capacity (J/m^3·℃), L is the latent heat (J/m^3) and z is the depth (m). Thus, q_h is the heat flux (J/m^2·s), q_w and q_v are the liquid and vapor water fluxes (m/s), respectively. k_h is thermal conductivity (W/m·℃), and C_w is the soil water heat capacity (J/m^3·℃). L_v is the latent heat of vaporization (J/m^3).

The upper boundary condition is defined as:

$$q_h(0) = -k_{ho} \frac{(T_s - T_1)}{\frac{\Delta z}{2}} + C_w (T_a - \Delta T_{pa}) q_{in} + L_v q_{vo} \qquad (2)$$

where k_{ho} is the conductivity of the soil surface organic material (W/m·℃), T_s is the soil surface temperature (℃), T_1 is the soil temperature of the first compartment (℃), ΔT_{pa} is the temperature difference between precipitation and air (℃), q_{vo} is the vapor water flow, and L_v is the latent heat (J/kg).

The lower boundary condition is defined as:

$$T_{LowB} = T_{amean} - T_{aamp}\, e^{-\frac{z}{d_a}} \cos((t - t_{ph})\omega - \frac{z}{d_a}) \qquad (3)$$

where t is time, t_{ph} is the phase shift, ω is the frequency, d_a is the damping depth, and T_{amean} and T_{aamp} are the mean and amplitude values of air temperature, respectively.

(b) Soil water flow.

Soil water is assumed to obey Darcy's law as generalized for unsaturated flow by Richards (1931), and the total flow q_w is the sum of the matrix flow, vapor flow and bypass flow:

$$q_w = -k_w(\frac{\partial \psi}{\partial z} - 1) - D_v \frac{\partial c_v}{\partial z} + q_{bypass} \quad (4)$$

where k_w is the unsaturated hydraulic conductivity (m/s), ψ is the water tension (m), z is depth (m), c_v is the concentration of vapor in soil air, D_v is the diffusion coefficient for vapor in the soil (m^2/s) and q_{bypass} is a bypass flow in the macro-pores (m/s).

(c) Surface energy balance approach.

Based on the law of energy conservation, the net radiation amounts to the latent heat flux, sensible heat flux and heat flux into soil:

$$R_{ns} = L_v E_s + H_s + q_h \quad (5)$$

where $L_v E_s$ is the latent heat (W/m^2), H_s is the sensible heat flux (W/m^2), and q_h is the heat flux into soil (W/m^2).

The latent heat flow is expressed as:

$$L_v E_s = \frac{\rho_a c_p}{\gamma} \frac{(e_{surf} - e_a)}{r_{as}} \quad (6)$$

where r_{as} is the aerodynamic resistance calculated as a function of wind and temperature gradients (s/m), e_{surf} is the vapor pressure at the land surface (Pa), e_a is the actual vapor pressure in the air (Pa), ρ_a is the air density (kg/m^3), c_p is the heat capacity of air (J/kg·℃), and γ is the psychrometric constant (kg/m^3).

Sensible heat flow is expressed as:

$$H_s = \rho_a c_p \frac{(T_s - T_a)}{r_{as}} \quad (7)$$

where T_s is the land surface temperature (℃), and T_a is the air temperature (℃).

(d) Snow dynamics.

Snow conditions are considered as a water storage and boundary condition for soil water flows and are an important factor influencing the soil heat boundary condition. Snow melting is based on the air temperature, global radiation and the heat flow from the soil:

$$M = M_T T_a + M_R R_{is} + \frac{f_{qh} q_h(0)}{L_f} \quad (8)$$

where R_{is} is global radiation, f_{qh} is a scaling coefficient, L_f is the latent heat of freezing, and $q_h(0)$ is the land surface heat flow. M_T is a temperature function and M_R is a function accounting for the influence of solar radiation.

$$M_T = \begin{cases} m_T & T_a \geq 0 \\ \frac{m_T}{\Delta z_{snow} m_f} & T_a < 0 \end{cases} \quad (9)$$

$$M_R = m_{R\,\min}(1 + s_1(1 - \mathrm{e}^{-s_2 s_{age}})) \quad (10)$$

where m_T, m_f, s_1, $m_{R\,\min}$ and s_2 are parameters. Δz_{snow} is the snow depth, which indicates that the refreezing efficiency is inversely proportional to snow depth. s_{age} is the age of surface snow.

In this study, the precision of this model is evaluated by Root Mean Square Error (*RMSE*), Mean Error (*ME*) and determination coefficient of linear regression (R^2) between the simulated and measured values. The calculation formulas are listed below:

$$RMSE = \sqrt{\frac{1}{N}\sum_{i=1}^{N}(C_i - M_i)^2} \quad (11)$$

$$ME = \frac{1}{N}\sum_{i=1}^{N}(C_i - M_i) \quad (12)$$

$$R^2 = 1 - \sum_{i=1}^{N}(C_i - M_i)^2 / (\sum_{i=1}^{N} M_i^{\,2} - (\sum_{i=1}^{N} M_i)^2) \quad (13)$$

where C_i and M_i are the simulated value and measured data, respectively. N is the number of observation samples. *RMSE* and *ME* represent the deviation of the simulated value from the observed value. Smaller absolute value represents better simulation accuracy. The coefficient of determination in linear regression, namely, R^2 represents the extent of correlation between simulated and measured values. An R^2 of 1 indicates that the simulated value perfectly fit the measured data.

2.2 Input data

Measurements were conducted from January 1st 2013 to December 31st 2013. The meteorological data used as the driving variables are the daily mean of air temperature (℃), precipitation (mm), relative humidity (%), global radiation (W/m^2), and wind speed (m/s), which were measured in the Beiluhe area. In 2013, the annual mean air temperature value was -3.29 ℃ and the annual precipitation value was 318.8 mm. Precipitation events in the Beiluhe area are concentrated in the period from May to September, and extreme precipitation events usually occur in July or August

(Yang et al. 2008). In this study, the maximum daily precipitation amounts in 2013 occurred on July 3rd 2013 and August 27th 2013, with amounts of 19.36 mm/day and 18.78 mm/day, respectively.

Except for some default parameters, the input parameters are listed as below. The latitude and altitude of the observation site are 34.51° and 4600 m, respectively. The wet and dry albedo are 0.25 and 0.35, respectively. The amplitude and mean values of air temperature are 16.40 and -3.29℃, respectively. The organic layer thickness is 0.1 m. The initial soil water contents and soil temperatures for each compartment measured in January 1st 2013 are input into the model. The calculation step is 24 hours and the simulation period is five years.

2.3 Model verification

2.3.1 Simulation of soil temperature

As shown in Figure 4, the results of shallow compartments (0.05-0.75 m) fit well through the comparison between the simulated and measured soil temperatures. The variation of simulated annual temperature cycling coincided closely with the measured data. The maximum discrepancy of

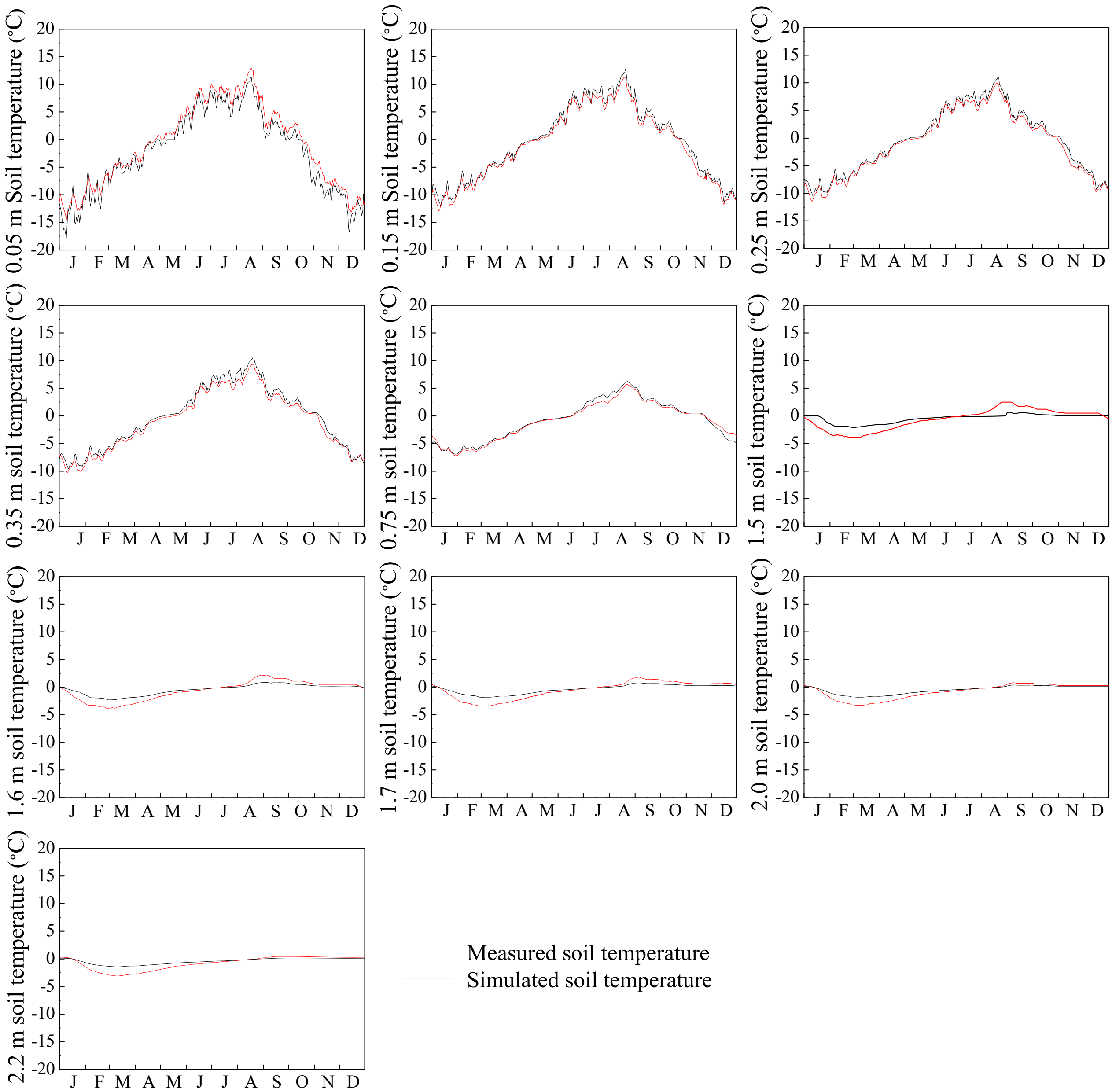

Figure 4 Comparison of measured and simulated daily mean soil temperatures at different depths.

the daily temperature value at each depth is approximately 3℃. As the depth increased, the year-round amplitude of simulated soil temperature gradually faded. The correlation extents are poor in lower compartments (0.75-2.2 m in Figure 4), but in actuality, the discrepancy between simulated and measured soil temperature is still under 3℃. In the shallow compartments, the simulated soil temperatures are lower than the measurements. However in lower compartments, the simulated soil temperatures in the first half of 2013 are higher than measured data; while in the second half of 2013, the simulated soil temperatures are lower than measurements. Apart from the minor defects above, the simulated and measured soil temperatures exhibit similarly annual sinusoidal variations, fading amplitudes with depth and synchronous appearance of the maximum. All in all, the result is fairly satisfactory for the entire soil profile.

Besides that, the summary statistics in Table 1 exhibit a convincing output. R^2 is greater than 0.6731, especially for the shallow compartments where R^2 is greater than 0.8825. From the top layer downwards, *RMSE* experiences a decline and the maximum is 2.9082, while *ME* increases from -1.7698 to 0.6038. For the simulation under complicated meteorological conditions in the Q-T Plateau, Timlin et al. (2002), Banimahd and Zand-Parsa (2013) suggested that the mean error is quite desirable when it is under 2℃.

2.3.2 Simulation of soil moisture content

The simulated soil water contents are quite consistent with the measured soil water contents (Figure 5). From June to October, namely, the warm season, the soil water content of shallow compartments (0.05-0.75 m) is approximately 4% higher than the measured data, while in frozen seasons, the simulated soil water content of shallow compartments is approximately 1% less than what was measured. In the lower compartments, except for the soil water content at 2 m and 2.2 m are remarkably higher in autumn, the simulated soil water content is approximately 4% higher than the measurements in the year round. In the start of thawing season, the measured soil water content is sharply increasing and then falling slowly in the shallow compartments. The simulated variation curve comparably flattens due to the imperfect consideration for water draining. Apart from these negligible discrepancies, the model can effectively simulate the delay of peak value for soil water content with soil depth.

As shown in Table 2, the *RMSE* and *ME* increased with depth, while the determination coefficient (R^2) decreased. R^2 of the shallow compartments are above 0.8570, *RMSE* are under 4.5973, and *ME* ranges from -2.4512 to 0.9430. Obviously, the difference between the simulated value and monitoring data increases from the shallow compartments to the lower compartments. *ME* between the simulated and measured soil water content in the thawed season is somewhat higher, which result from the poor consideration for frequent precipitation in summer on the Q-T plateau. While in the lower compartments (below 0.75 m), the difference between simulated and measured soil water content is completely different, avoiding from the influence of dramatically varied seasonal precipitation. This interesting phenomenon also indicates that the rain water cannot reach deeper compartments, especially those deeper than 0.75 m. In summary, the

Table 1 Summary statistics of discrepancy between simulated and measured soil temperatures

Depth (m)	Simulated mean (℃)	Measured mean (℃)	R^2	RMSE (℃)	ME (℃)
0.05	-2.3722	-0.1084	0.9396	2.9082	-2.2639
0.15	-2.2392	-0.4693	0.9578	2.2307	-1.7698
0.25	-2.0863	-0.4827	0.9639	1.9471	-1.6036
0.35	-1.9377	-0.2230	0.9637	2.0380	-1.7148
0.75	-1.2105	-0.7815	0.8825	1.3183	-0.4291
1.5	-0.4546	-0.5956	0.8668	1.1592	0.1410
1.6	-0.3129	-0.6206	0.7918	1.3664	0.3077
1.7	-0.2223	-0.5296	0.8353	1.2998	0.3073
2	-0.1863	-0.7893	0.7060	1.3029	0.6031
2.2	-0.1722	-0.7760	0.6731	1.2374	0.6038

Table 2 Summary statistics of discrepancy between simulated and measured soil water content

Depth (m)	Simulated mean (%)	Measured mean (%)	R^2	RMSE (%)	ME (%)
0.05	9.9905	9.1546	0.9318	2.1710	0.8358
0.15	10.1975	11.5110	0.9151	2.2318	0.8501
0.25	9.6175	8.6745	0.9089	2.2021	0.9430
0.35	9.7321	9.9730	0.9082	2.1884	0.7591
0.75	11.2215	10.9218	0.8570	2.1635	0.2997
1.5	7.8961	11.2251	0.8447	3.5547	-3.3290
1.6	8.1549	11.3922	0.8191	3.5509	-3.2374
1.7	8.2334	11.8202	0.7412	3.9271	-3.5868
2	9.4123	12.1219	0.6373	4.5973	-3.7095
2.2	9.8723	12.3235	0.5587	3.8958	-2.4512

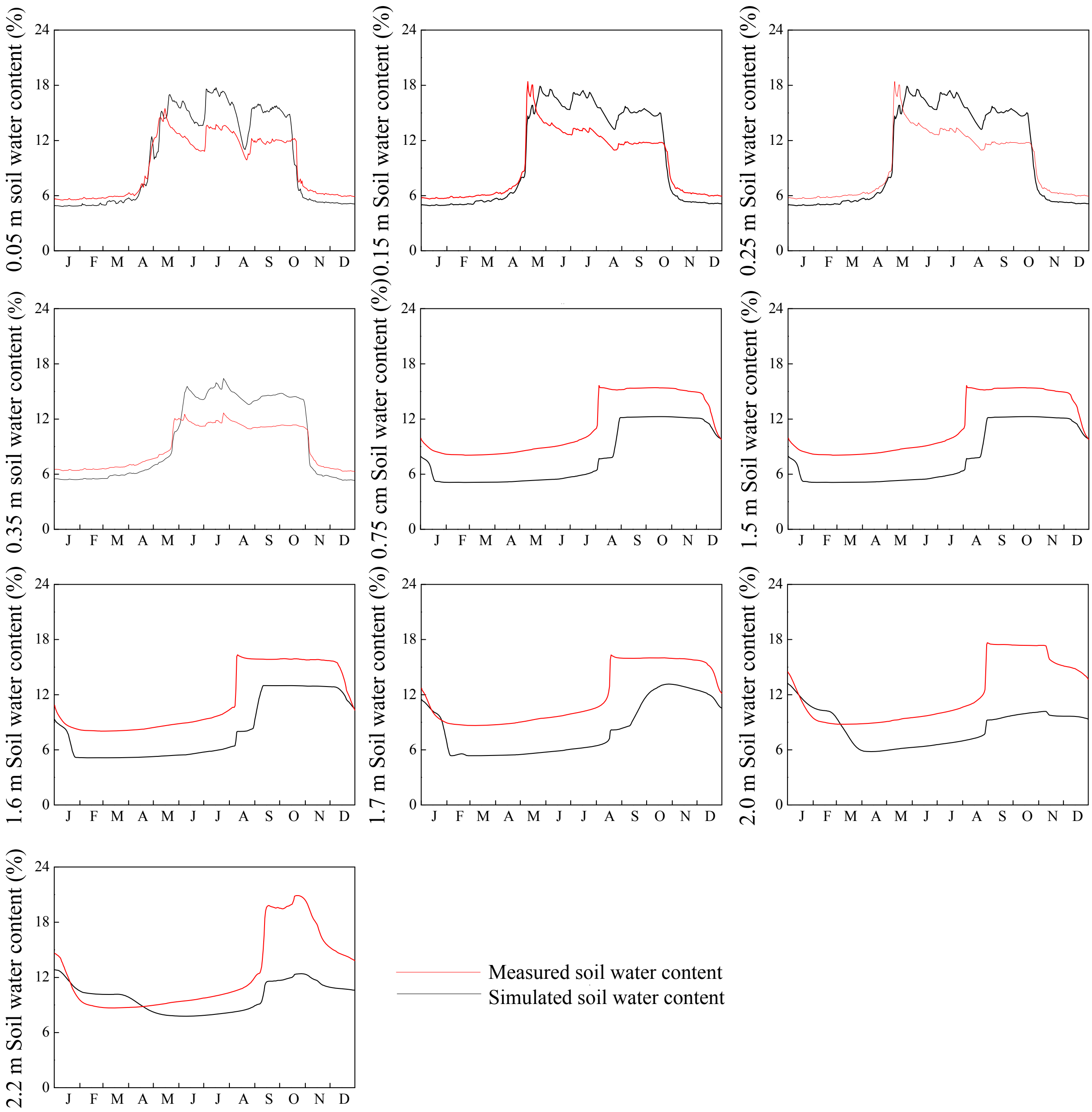

Figure 5 Comparison of measured and simulated daily mean soil water content at different depths.

simulation of soil water content is quite desirable.

2.3.3 Simulation of heat flux

Figure 6 shows the comparison between the simulated and measured soil heat fluxes at depths of 0.05 m and 0.15 m. It is clear that the simulated soil heat flux coincided with measured data for the entire observed period. The only deficiency of the simulation result is that the variation in the diurnal amplitude of the soil heat flux was comparatively weaker. This difference is also shown in Table 3, the absolute mean of *ME* is small, whereas the *RMSE* is somewhat higher. With an excellent outcome for R^2, it is concluded that the simulation for soil heat flux is perfect. Considering the good accuracy, the heat flux could be an important indicator for the prediction of soil thermal state. Using the heat flux to explore the variations of the active layer's thermal state under climatic change conditions will be convincible.

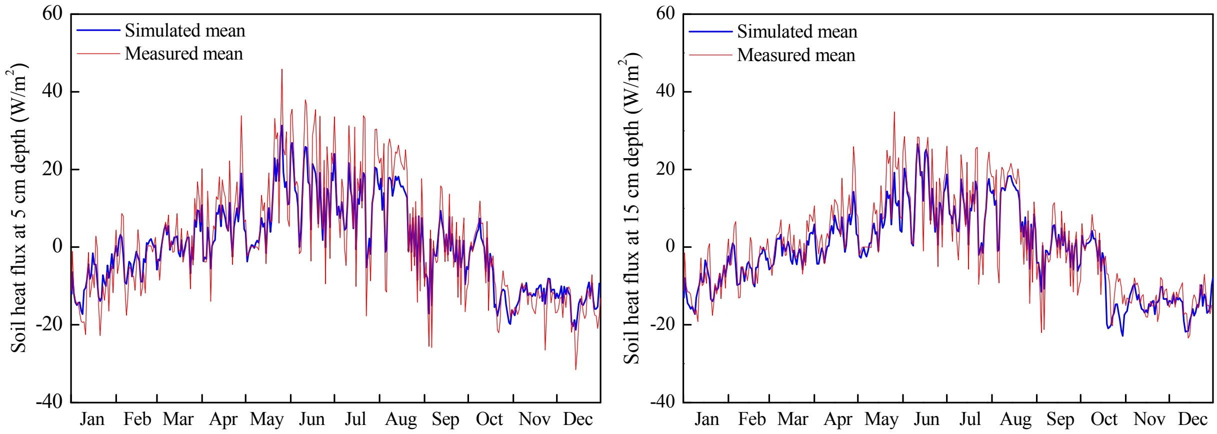

Figure 6 Comparison of measured and simulated soil heat flux at depths of 0.05 m and 0.15 m.

2.4 Model application

The successful validation facilitated the application of the varied atmospheric data into the model above. The accumulated precipitation amount in 2013, i.e. the research period, is 318.8 mm/a. While the mean accumulated precipitation of recent 10 years in Beiluhe area is 388 mm/a, and the extremely high accumulated precipitation emerged in 2011, with the accumulated precipitation amount of 495 mm/a. The mean accumulated precipitation amount of recent 10 years is approximately a quarter more than the accumulated precipitation amount in 2013, the maximum accumulated precipitation amount in recent 10 years is approximately a half more than the accumulated precipitation amount in 2013. Therefore, the year-round precipitation amount input into the predicted model were increased by 25% and 50% for 1.25P and 1.5P, respectively. Through linear regression, the precipitation amount has a trend to increase by 3.8 mm/a, even the accumulated precipitation amount in research period (2013) is almost the minimum in recent 10 years (Figure 7). So, the accumulated precipitation amounts for 1.25P and 1.5P have potential to emerge again in long term, due to its appearance in merely recent 10 years. The annual increased precipitation amounts, with other atmospheric data unchanged, were applied into the model again. The reliable prediction of the permafrost active layer's thermal state under the effect of increasing precipitation at the Q-T plateau was obtained.

Table 3 Summary statistics of discrepancy between simulated and measured soil heat flux

Depth (m)	Simulated mean (W/m^2)	Measured mean (W/m^2)	R^2	RMSE (W/m^2)	ME (W/m^2)
0.05	0.5186	-1.0410	0.9176	5.4224	-0.8552
0.15	1.3738	0.5907	0.8879	4.4467	-1.6316

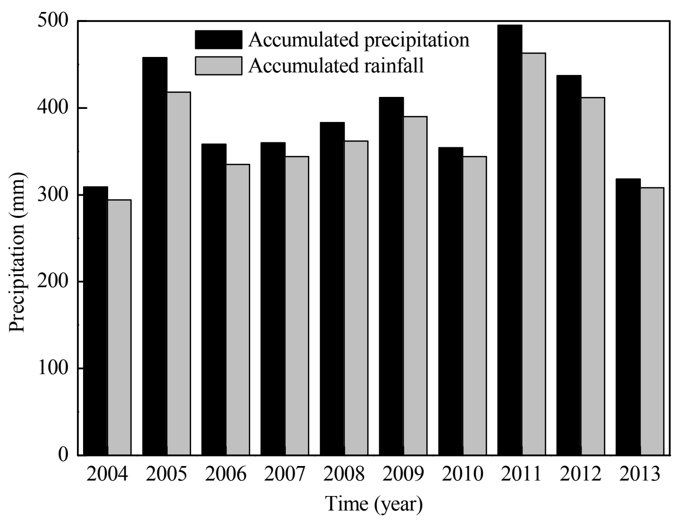

Figure 7 Accumulated precipitation and accumulated rainfall in recent 10 years.

3 Results

3.1 Prediction of soil temperature under increased precipitation

The soil temperature for three different conditions is very close, which means the increased precipitation didn't influence the temperature much from macro perspective in the model. As shown in Figure 8, the two thermal contours are very similar, and the 0℃ isotherms are almost identical. So, it is required to analyze the energy budget at land surface in order to research whether active layer has gained or lost energy. Then the changing trend of soil thermal state in the long run could be obtained. Therefore, the analysis of soil surface heat flux budget is especially important.

3.2 Prediction of soil heat flux under increased precipitation

From the comparison between simulated and measured soil temperature, soil water content and soil heat flux, it is found that the simulation of the soil heat flux is the most accurate. Apart from the moderately weaker diurnal cycle, this model can perfectly reproduce the shallow soil heat flux. Therefore, the change in soil heat flux is used as an indicator to detect the subtle change of thermal state in permafrost active layer under the effects of increased precipitation.

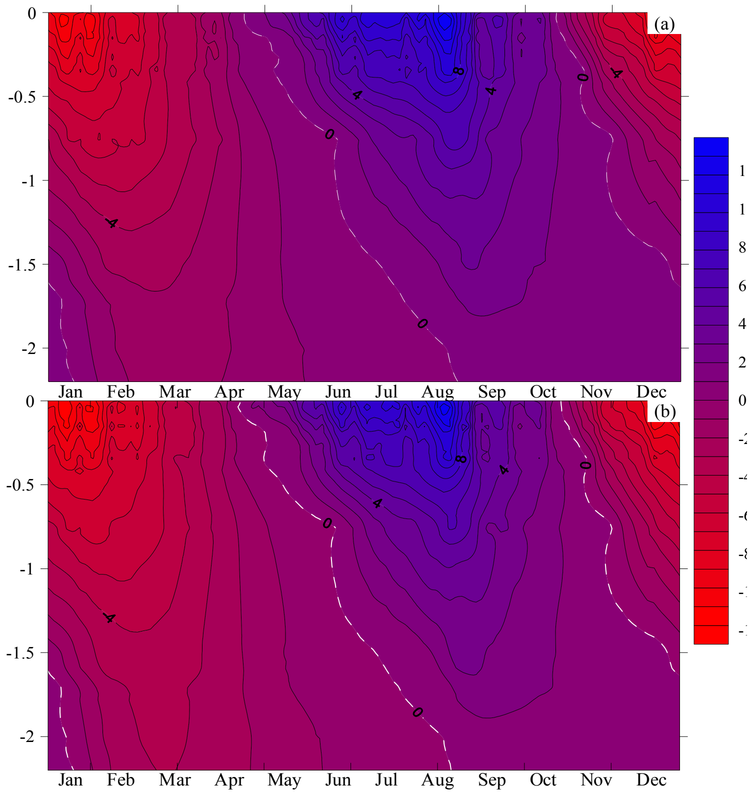

Figure 8 Predicted isotherms. The isotherm of (a) and (b) are based on the simulated soil temperature under the condition P and 1.5P, respectively. (The P condition means precipitation unchanged and 1.5P condition means precipitation was increased by a half.)

As shown in Figure 9, the soil surface heat fluxes under three precipitation patterns are drawn with different colors, while the precipitation amount of the three patterns was only left with the unchanged precipitation amount for explicit illustration. The effect of precipitation on the soil surface heat flux varies with the season alternation, which promotes the analysis of the effect of increased precipitation amount on the thermal dynamics of the active layer in a particular season. Only in this way can we summarize the laws and mechanisms of how changing precipitation affects the permafrost active layer.

There is no difference in surface heat flux in spring and autumn under different precipitation patterns, three lines almost overlapped in Figure 9 (a) and (c), which means increased rainfall amount does not influence soil surface heat flux obviously. In summer and winter, however, the increa sed precipitation amount of some precipitation events may trigger a heat flux disturbance. These events in Beiluhe area were summarized as: (1) extreme precipitation events in summer, namely, heavy rainfall or longer duration rainfall; (2) snowfall in winter.

As shown in Figure 9 (b), the precipitation amount on July 3rd, 2013 reached 19.36 mm/day, while the rainfall capacities of 1.25P and 1.5P reached 24.20 mm/day and 29.04 mm/day, respectively. The soil surface heat flux showed a positive correlation with rainfall amount: the soil surface heat flux increased from 16.94 W/m^2 (P) to 18.33 W/m^2 (1.25P) and 18.51 W/m^2 (1.5P), respectively. A Soil Surface Heat Flux below zero means that the active layer releases heat. In other words, the influence from extreme rainfall events in summer leads to an increase in the incoming heat flux, caused by the infiltrated water bringing more energy into the permafrost active layer. In actuality, increased rainfall amount brings more water into the permafrost active layer and deepens the infiltration depth of rainfall water. Therefore, the additional energy, accompanied with the infiltrating water, warmed the active layer and

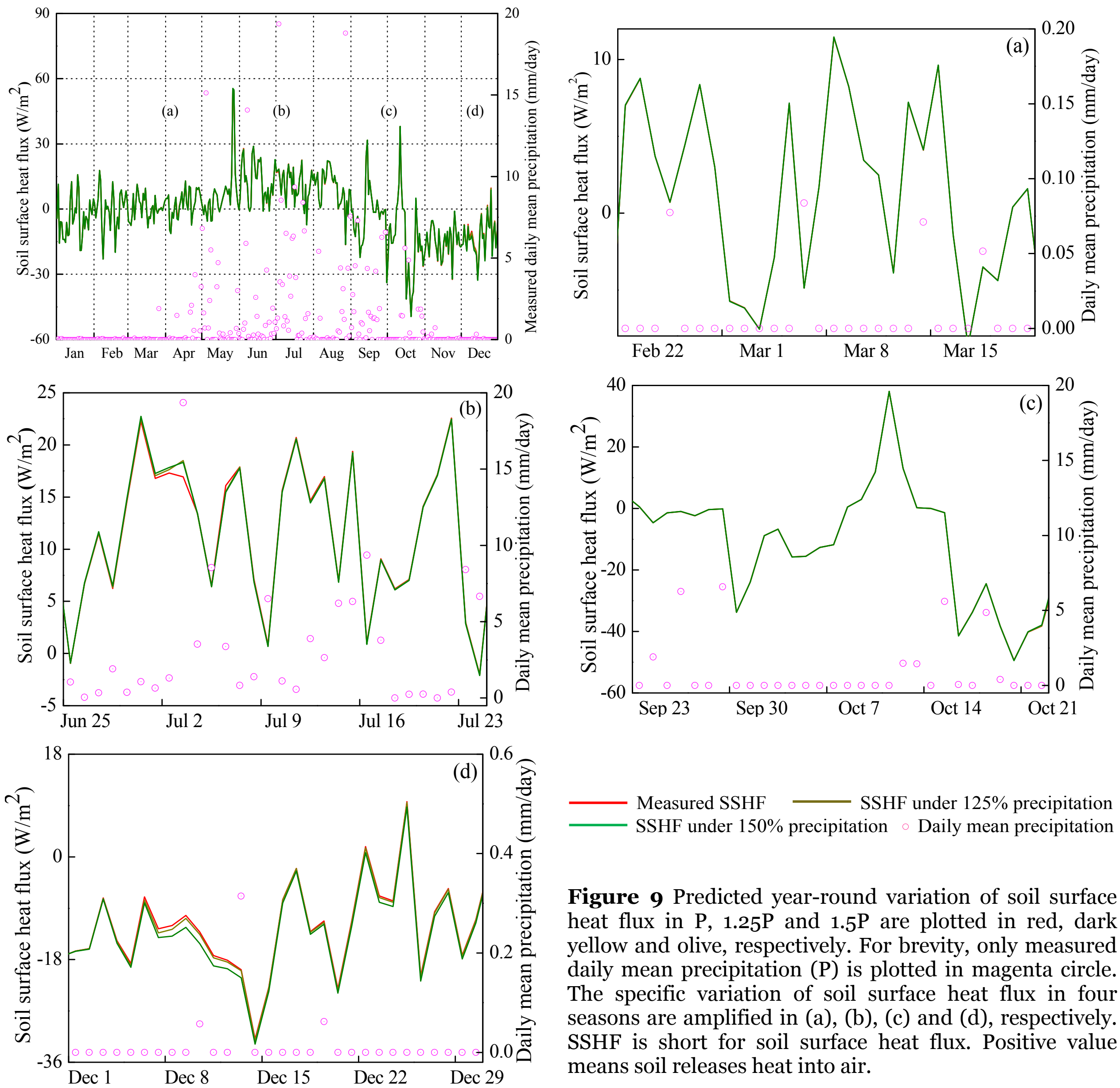

Figure 9 Predicted year-round variation of soil surface heat flux in P, 1.25P and 1.5P are plotted in red, dark yellow and olive, respectively. For brevity, only measured daily mean precipitation (P) is plotted in magenta circle. The specific variation of soil surface heat flux in four seasons are amplified in (a), (b), (c) and (d), respectively. SSHF is short for soil surface heat flux. Positive value means soil releases heat into air.

accelerated the degradation of permafrost.

As shown in Figure 9 (d), the precipitation amount on December 10th, 2013 was only 0.10 mm/day, so the precipitation amount of 1.25P and 1.5P were 0.13 mm and 0.150 mm, respectively, and the soil surface heat flux decreased with increasing rainfall amount, dropping from -13.16 W/m^2 (P) to -13.61 W/m^2 (1.25P) and -15.20 W/m^2 (1.5P). It is known that a negative value of soil surface heat flux means that the active layer releases heat outwards. The intensified precipitation, which is snowfall in the frozen season, decreased the soil surface heat flux, which indicates that more snowfall made the active layer release more heat outwards and promoted the development of permafrost in the frozen season. Snowfall in the frozen season accumulated on the soil surface and resembled the insulating cover, which prevented the solar energy from penetrating into the active layer. The snow cover formed on the soil surface reflected solar radiation and absorbed the heat of phase changes released from the active layer. This phenomenon provides another simulated demonstration for the thermal insulation effect of snow cover (Luetschg 2005; Zhang et al. 2001).

Recent studies indicate that increased precipitation tends to occur in the thawed season, it means the effect from snow cover is limited, especially in Q-T Plateau. It is widely accepted that global warming and high radiation will intensify the extreme precipitation (Chung and Power 2015; Utsumi et al. 2011), therefore, the warming effect of increased summer rainfall also deserves attention. Overall, regardless of the small change in soil heat flux under increased amounts of precipitation, the wetting climate trend in the Q-T Plateau has less influence on the thermal dynamic of the permafrost active layer than global warming, the thermal state responds to the changes in air temperature, solar elevation angle and global radiation more violently. While in the long term, the wetting trend of climate still plays an important role in the thermal state of permafrost active layer.

4 Discussion

Based on the comparison between simulated and measured data, the application of the CoupModel in this study is convincing, and the simulated results are quite satisfactory. Using finite atmospheric data, the hydro-thermal dynamics of the permafrost active layer can be satisfactorily reproduced. Previous researchers successfully applied the CoupModel to the simulation of the hydro-thermal state of active layers in other area of the Q-T plateau (Hu et al. 2015; Zhou et al. 2013). When introduced to the Beiluhe area, the selection of specific parameters needs time to calibrate and update. Determining more accurate soil characteristics of each compartment and selecting input parameters suitable for the Q-T plateau area could significantly improve the simulation accuracy.

From these results, it is found that the simulation results are quite satisfactory for thermal data, especially for the soil surface heat flux. An accurate simulation guarantees the reliability of the prediction for the thermal state of the active layer under increased precipitation patterns. Even though the simulation of soil water content is fairly poor, the precision of the simulated active layer's hydrological state under constantly changing meteorological conditions at the Q-T plateau is quite desirable (Zhang et al. 2016). Furthermore, the simulation precision has improved compared to previous models used in this area. The defect in the simulated water content is also obvious: in shallow compartments (0.05-0.75 m), the simulated water contents are much higher than those measured in the thawed season and relatively smaller than the measured in the frozen season. While in lower compartments, the simulated water contents are lower than the measured data overall. This deviation may result from the improper selection of hydraulic parameters.

Concerning the predicted results, the most important finding deviating from former researches is that the increased precipitation in different seasons disturbed the ground heat flux with different effects. It is believed that the winter precipitation lowering the soil temperature and soil surface heat flux through monitoring analysis (Wen et al. 2014), and in the simulation the increased precipitation also reduced the soil surface heat flux. The summer rainfall is believed to lower the soil temperature and soil surface heat flux through monitoring analysis too (Wen et al. 2014), while in the simulation, the increased precipitation elevated the soil surface heat flux compared with the unchanged precipitation pattern. In other words, the monitoring analysis indicated that precipitation events cool the active layer both in summer and winter. Based on comparative analysis, the simulated results indicated the increased precipitation in the Q-T plateau further cools the active layer in winter but warms it in summer. Thus in the predicted model, inconspicuous variation of the active layer's thickness under increased precipitation (Figure 8) is partly attributed to that contradictory effect, the warming effect in summer offsets the cooling effect in winter to some extent.

As previous researches indicate, the climate at the Q-T plateau trends towards more precipitation. More importantly, the increased precipitation is concentrated in the thawed season. To explore the seasonal variation of precipitation on the active layer thickness and its thermal state, we encourage adding some working conditions to the simulation: for example, raising precipitation amounts in the thawed season and keep the precipitation in the frozen season unchanged, vice or versa. Under these circumstances, a different conclusion for wetting trends of the climate in the Q-T plateau area may be obtained.

However, the model was only applied to a single point in Q-T plateau, and the measured data were only from one year in this study. Further studies should concentrate more heavily on using simulations with long-term measured data from different sites in the Q-T Plateau.

5 Conclusions

Based on the above analysis and discussion of the simulated active layer thermal state under increased precipitation, some conclusions are summarized as follows:

(1) The results in this study demonstrated that the CoupModel could accurately model the hydro-thermal transfer process and land surface energy balance of the active layer in permafrost regions in the Qinghai-Tibet Plateau. With this model, the variations of land ground heat flux and active layer thickness under the circumstances of increased seasonal precipitation were successfully predicted.

(2) While the variation of active layer thickness is almost negligible, the soil surface heat flux does change under extreme rainfall events in summer and sparse precipitation in winter. Furthermore, the effects of these precipitation events differ distinctively in different seasons.

(3) The results show that a precipitation increasement of 25% or 50% on July 3rd 2017 increased the soil surface heat flux by 1.39 W/m^2 or 1.57 W/m^2, respectively, while a precipitation increasement of 25% or 50% on December 10th decreased the surface heat flux by 0.45 W/m^2 or 2.04 W/m^2, respectively, to its maximum extent.

(4) The comparison of different precipitation patterns indicates that increased precipitation in summer warms the active layer. Increased precipitation in winter cools the active layer, which coincides with the cooling effects of snow cover.

Acknowledgements

The author would like to thank the National Natural Science Foundation of China (Grant Nos. 41771073, 41871061, 41690144 and 41530639), the Major Program of Bureau of International Cooperation, the Chinese Academy of Sciences (131B62KYSB20170012) and Open Fund of State Key Laboratory of Frozen Soil Engineering (Grant No. SKLFSE201712) for financially supporting this research.

References

Anisimov OA, Shiklomanov NI, Nelson FE (1997) Global warming and active-layer thickness: results from transient general circulation models. Global and Planetary Change 15 (3-4): 61-77. https://doi.org/10.1016/S0921-8181(97)00009-X

Banimahd SA, Zand-Parsa S (2013) Simulation of evaporation, coupled liquid water, water vapor and heat transport through the soil medium. Agricultural Water Management 130: 168-177. http://doi.org/10.1016/j.agwat.2013.08.022

Chung CTY, Power SB (2016) Modelled impact of global warming on ENSO-driven precipitation changes in the tropical Pacific. Climate Dynamics 47(3-4): 1303-1323. http://doi.org/10.1007/s00382-015-2902-9

Luetschg M, Haeberli W (2005) Permafrost evolution in the Swiss Alps in a changing climate and the role of the snow cover. Norsk Geografisk Tidsskrift - Norwegian Journal of Geography 59(2): 78-83. http://doi.org/10.1080/00291950510020583

Hollesen J, Elberling B, Jansson PE (2011) Future active layer dynamics and carbon dioxide production from thawing permafrost layers in Northeast Greenland. Global Change Biology 17(2): 911-926. http://doi.org/10.1111/j.1365-2486.2010.02256.x

Hu G, Zhao L, Wu X, et al. (2015) Modeling permafrost properties in the Qinghai-Xizang (Tibet) Plateau. Science China Earth Sciences 58(12): 2309-2326. http://doi.org/10.1007/s11430-015-5197-0

Iijima Y, Fedorov AN, Park H, et al. (2010) Abrupt increases in soil temperatures following increased precipitation in a permafrost region, central Lena River basin, Russia. Permafrost & Periglacial Processes 21(1): 30-41. http://doi.org/10.1002/ppp.662

Jansson PE (1991) Simulation model for soil water and heat conditions. Description of the SOIL model. Communications Division of Agricultural Hydrotechnics Swedish University of Agricultural Sciences.

Jansson PE, Karlberg L (2004) Theory and practice of coupled heat and mass transfer model for soil-plant-atmosphere system (In Chinese). In: Zhang HJ, Cheng JH, Wang W. Translation. Beijing: Science Press.

Jansson PE, Moon D (2001) A coupled model of water, heat and mass transfer using object orientation to improve flexibility and functionality. Environmental Modelling and Software 16: 37-46

Jin H, Chang X, Wang S (2007) Evolution of permafrost on the Qinghai - Xizang (Tibet) Plateau since the end of the late Pleistocene. Journal of Geophysical Research Earth Surface 112(F2). http://doi.org/10.1029/2006JF000521

Johnsson H, Jansson PE (1993) SOILN model -Technical description of soilprocesses and the simple plant uptake function. Department of Soil Sciences, Swedish University of Agricultural Sciences, Uppsala.

Kokelj SV, Tunnicliffe J, Lacelle D, et al. (2015) Increased precipitation drives mega slump development and destabilization of ice-rich permafrost terrain, northwestern Canada. Global & Planetary Change 129: 56-68. http://doi.org/10.1016/j.gloplacha.2015.02.008

Koven CD, Ringeval B, Friedlingstein P, et al. (2011) Permafrost carbon-climate feedbacks accelerate global warming.

Proceedings of the National Academy of Sciences of the United States of America 108(36): 14769-14774. http://doi.org/10.1073/pnas.1103910108
Kroener E, Vallati A, Bittelli M (2014) Numerical simulation of coupled heat, liquid water and water vapor in soils for heat dissipation of underground electrical power cables. Applied Thermal Engineering 70(1): 510-523. http://doi.org/10.1016/j.applthermaleng.2014.05.033
Ling F, Zhang T (2003) Impact of the timing and duration of seasonal snow cover on the active layer and permafrost in the Alaskan Arctic. Permafrost & Periglacial Processes 14(2): 141-150. http://doi.org/10.1002/ppp.445
Ma W, Liu D, Wu Q (2008) Monitoring and analysis of embankment deformation in permafrost regions of Qinghai-Tibet Railway. Rock & Soil Mechanics 29(3): 571-579. (In Chinese with English abstract) http://doi.org/10.16285/j.rsm.2008.03.005
Nelson F, Shiklomanov N, Hinkel K, et al. (2004) The Circumpolar Active Layer Monitoring (CALM) Workshop and THE CALM II Program. Polar Geography 28(4): 253-266. http://doi.org/10.1080/789610205
Richards LA (1931) Capillary conduction of liquids through porous Mediums. Physics 1(5): 318-333. http://doi.org/10.1063/1.1745010
Rockström J, Jansson PE, Barron J (1998) Seasonal rainfall partitioning under runon and runoff conditions on sandy soil in Niger. On-farm measurements and water balance modelling. Journal of Hydrology 210(1-4): 68-92. http://doi.org/10.1016/s0022-1694(98)00176-0
Schuur EA, Mcguire AD, Schädel C, et al. (2015) Climate change and the permafrost carbon feedback. Nature 520(7546): 171-179. http://doi.org/10.1038/nature14338
Stendel M, Christensen JH (2002) Impact of global warming on permafrost conditions in a coupled GCM. Geophysical Research Letters 29(13): 10-1-10-4. http://doi.org/10.1029/2001GL014345
Stieglitz M, Déry SJ, Romanovsky VE, et al. (2003) The role of snow cover in the warming of arctic permafrost. Geophysical Research Letters 30(13): 1721. http://doi.org/10.1029/2003GL017337
Timlin DJ, Pachepsky Y, Acock BA, et al. (2002) Error analysis of soil temperature simulations using measured and estimated hourly weather data with 2DSOIL. Agricultural Systems 72(3): 215-239. http://doi.org/10.1016/S0308-521X(01)00075-0
Utsumi N, Seto S, Kanae S, et al. (2011) Does higher surface temperature intensify extreme precipitation? Geophysical Research Letters 38(16): 239-255. http:// doi.org/10.1029/2011GL048426
Wen Z, Niu F, Yu Q, et al. (2014) The role of rainfall in the thermal-moisture dynamics of the active layer at Beiluhe of Qinghai-Tibetan plateau. Environmental Earth Sciences 71(3): 1195-1204. http://doi.org/10.1007/s12665-013-2523-8
Wu Q, Hou Y, Yun H, et al. (2015) Changes in active-layer thickness and near-surface permafrost between 2002 and 2012 in alpine ecosystems, Qinghai–Xizang (Tibet) Plateau, China. Global & Planetary Change 124: 149-155. http://doi.org/10.1016/j.gloplacha.2014.09.002
Yang M, Yao T, Gou X, et al. (2008) Precipitation distribution along the Qinghai-Xizang (Tibetan) Highway, Summer 1998. Arctic Antarctic & Alpine Research 40(4): 761-769. http://doi.org/10.1657/1523-0430(06-058)%5BYANG%5D2.0.CO;2
Zhang M, Wen Z, Xue K, et al. (2016) A coupled model for liquid water, water vapor and heat transport of saturated–unsaturated soil in cold regions: model formulation and verification. Environmental Earth Sciences 75: 701. http://doi.org/10.1007/s12665-016-5499-3
Zhang T. (2005) Influence of the seasonal snow cover on the ground thermal regime: An overview. Reviews of Geophysics 43(4):RG4002. http://doi.org/10.1029/2004RG000157
Zhang T, Barry RG, Haeberli W (2001) Numerical simulations of the influence of the seasonal snow cover on the occurrence of permafrost at high latitudes. Norsk Geografisk Tidsskrift - Norwegian Journal of Geography 55(4): 261-266. http://doi.org/10.1080/00291950152746621
Zhao L, Sheng Y, Wu T, et al. (2013) Permafrost Distribution and Thermal Dynamics over the Tibetan Plateau, China. AGU Spring Meeting. AGU Spring Meeting Abstract, 2013.
Zhou J, Kinzelbach W, Cheng G, et al. (2013) Monitoring and modeling the influence of snow pack and organic soil on a permafrost active layer, Qinghai–Tibetan Plateau of China. Cold Regions Science & Technology 90-91: 38-52. http://doi.org/10.1016/j.coldregions.2013.03.003
Zhou Z, Yi S, Chen J, et al. (2017) Responses of alpine grassland to climate warming and permafrost thawing in two basins with different precipitation regimes on the Qinghai-Tibetan Plateaus. Arctic Antarctic & Alpine Research 47(1): 125-131. http://doi.org/10.1657/AAAR0013-098
Zhu X, Wu T, Li R, et al. (2017) Impacts of summer extreme precipitation events on the hydrothermal dynamics of the active layer in the Tanggula permafrost region on the Qinghai - Tibet Plateau. Journal of Geophysical Research Atmospheres.122(21): 11, 549-11, 567. http://doi.org/10.1002/2017JD026736
Zhu Z, Li Y, Xue C (2011) Changing tendency of precipitation in permafrost regions along Qinghai-Tibet railway during last thirty years. Journal of Glaciology & Geocryology 33: 846-850. (in Chinese with English abstract)
Zimov SA, Schuur EA, Chapin FS (2006) Climate change. Permafrost and the global carbon budget. Science 312(5780): 1612-1613. http://doi.org/10.1126/science.1128908